

Study on Properties of Plasmonic Waveguide of Graphene-Coated Nanotube with a Dielectric Substrate

MIAO SUN (✉ 281452063@qq.com)

Chongqing Normal University <https://orcid.org/0000-0002-2269-9540>

Zhuanling He

National University of Defense Technology

Libing Huang

Chongqing Normal University

Research Article

Keywords: Waveguides, Graphene, Surface plasmonic, Transmission properties

Posted Date: February 8th, 2022

DOI: <https://doi.org/10.21203/rs.3.rs-1195798/v1>

License:   This work is licensed under a Creative Commons Attribution 4.0 International License.

[Read Full License](#)

Abstract

A hybrid plasmonic waveguide structure composed of graphene-coated nanotube with a dielectric substrate is proposed in this paper. Transmission properties of the fundamental mode are studied by the finite element method (FEM). The results reveal that the mode transmission properties are greatly dependent on the nanotube radius and internal-external diameter ratio, gap distance, nanotube permittivity, as well as chemical potential of graphene. Meanwhile, it is compared with the graphene-coated nanowires with a dielectric substrate [40]. By optimizing the parameters, the structure could achieve long-range propagation with the propagation length about 12.56 μm . Moreover, it could realize deep-subwavelength confinement with the normalized mode area only $\sim 10^{-7}$. This structure may offer certain theoretical basis for integrated nanophotonic devices to achieve long-distance transmission in the deep-subwavelength range.

1 Introduction

Surface plasmons (SPs) [1–3] are the surface electromagnetic wave propagating at the interface between a metal and a dielectric. Because of breaking through the diffraction limit and controlling light at subwavelength scale, SPs have attracted extensive attention of scholars worldwide and developed rapidly [4–8]. Usually, noble metals are used to stimulate and support surface plasmons (SPs). Various metal-based SPs waveguides have been proposed [9–23]. However, the metal-based SPs waveguides usually suffer from large ohmic loss and weak field confinement in the mid-infrared (mid-IR) to terahertz (THz) frequency range [24].

Recently, it has been found that graphene can exhibit “metal-like” properties in mid-infrared (mid-IR) to terahertz (THz) wavelengths [25], which can stimulate SPs. Compared to metal SPs, graphene SPs has the advantages of low propagation loss, tight field confinement and tunable electromagnetic properties [26–27]. Therefore, a large number of graphene SPs devices have been proposed, such as graphene nanoribbon waveguide [28–29], graphene nanowire waveguide [30–31], slot/wedge waveguide [32], hybrid waveguide [33–34], and modulator [35–36]. Among them, the hybrid waveguide has a better tradeoff between strong field confinement and low propagation loss, which has been widely studied in recent years. The graphene-coated nanowire waveguide [37–44] is a research hotspot in hybrid waveguides because of its simple structure, easy fabrication and no cut-off of fundamental mode. It has been shown that the graphene-coated nanowire waveguide has stronger field confinement than the metal nanowire waveguide, and the normalized mode area is about 10^{-3} [37]. In order to further improve the field confinement and reduce the mode propagation loss, researchers have proposed a graphene-based cylindrical hybrid waveguide [38–39] and the graphene-coated nanowire waveguide with dielectric substrate [40–42]. In reference [38], although the normalized mode area of the graphene-based cylindrical waveguide is reduced to 10^{-6} , the propagation distance is less than 2 μm . In reference [40], the propagation loss of the graphene-coated nanowire waveguides with dielectric substrate is smaller, and the propagation distance is about 7 μm . But the mode confinement is also reduced, and the mode area is one order of magnitude larger than the former.

Considering the advantages of the hybrid plasmonic waveguide, a new type of plasmonic waveguide structure composed of the graphene-coated nanotube with the dielectric substrate is designed in this paper. The graphene-coated nanotube waveguide structure has not been reported in related studies, and it has better performance than graphene-coated nanowire waveguide structure. The fundamental mode transmission properties of the waveguide are analyzed in detail by the finite element method. By adjusting the geometric parameters and electromagnetic parameters, the transmission properties are optimized. At the same time, the transmission properties are compared with that of the graphene-coated nanowire waveguides with the dielectric substrate [40]. It is found that the proposed waveguide has long propagation length and small mode area, which has important application value in the field of integrated nanophotonic devices.

2 Model And Theory

Figure 1 presents a two-dimensional structural diagram of the proposed waveguide, which consists of monolayer graphene layer and dielectric nanotube as well as rectangle dielectric substrate. The studied structure is embedded in air. The inner and outer radii of the dielectric nanotube are r_i and r_o with the ratio $S_1(S_1=r_i/r_o)$. The inner filling media and outer filling media of the nanotubes are different, and their permittivities are ϵ_i and ϵ_o . The outer layer of the rectangular dielectric substrate is also filled with the medium (with a height of h_o and a width of w_o), and the inner layer of the rectangular dielectric substrate is filled with the medium (with a height of h_i and a width of w_i). The height/width ratio of inner and outer layers of the rectangular dielectric substrate is $S_2(S_2=h_i/h_o=w_i/w_o)$. Considering the large loss of high index, the interiors of nanotube and rectangular dielectric substrate are filled with air ($\epsilon_1 = 1$). The gap height between the graphene-coated nanotube and the rectangular dielectric substrate is g . Graphene is wrapped in the outer layer of the dielectric nanotube, which can be achieved by chemical vapor deposition of Vander Ed Ley. In the mid infrared frequency range, the permittivity of graphene [43] can be calculated by the following formula:

$$\epsilon_g = 1 + \frac{i\sigma(\omega)}{\omega\epsilon_0\Delta}$$

1

Where $\Delta = 0.335\text{nm}$ is the thickness of single layer graphene [40], ω is the radiation angle frequency of incident light, and ϵ_0 is the vacuum dielectric constant. $\sigma(\omega)$ is the surface conductivity of the graphene film, which can be derived from the famous Kubo's formula, [44, 45]:

$$\sigma(\omega) = \sigma_{\text{int } ra} + \sigma_{\text{int } er}$$

2

$$\sigma(\omega)_{\text{int } ra} = \frac{2ie^2k_B T}{\pi\hbar^2(\omega + i\tau^{-1})} \ln \left[2\cosh \left(\frac{\mu_c}{2k_B T} \right) \right]$$

3

$$\sigma(\omega)_{\text{int } er} = \frac{e^2}{4\hbar} \left[\frac{1}{2} + \frac{1}{\pi} \arctan \left(\frac{\hbar\omega - 2\mu_c}{2k_B T} \right) - \frac{i}{2\pi} \ln \frac{(\hbar\omega + 2\mu_c)^2}{(\hbar\omega - 2\mu_c)^2 + 4(k_B T)^2} \right]$$

4

Where $\sigma_{\text{int } ra}$ is the intraband conductivity of graphene and $\sigma_{\text{int } er}$ is the interband conductivity of graphene. Here, the temperature $T = 300\text{K}$, the charge of the electron $e = 1.6 \times 10^{-19}\text{C}$, the relaxation time $\tau = 0.5\text{ps}$ [46], \hbar is the reduced plank constant, k_B is the Boltzmann's constant, and μ_c is the chemical potential of graphene. It can be seen from the above formula that the conductivity of graphene changes with changing the frequency and chemical potential.

Because the waveguide structure proposed in this paper is complex, it is not easy to directly solve the wave equation to calculate the mode properties. Therefore, the COMSOL Multiphysics software based on the finite element method is used to calculate the mode transmission properties of the waveguide. In the process of numerical simulation, graphene is treated as an ultra-thin film with surface conductivity of $\sigma(\omega)$. The effective refractive index is defined as $n_{\text{eff}} = \beta/k_0$, where β is the propagation constant which can be obtained directly by COMSOL software and k_0 is the wavenumber in free space; the propagation length can be defined by $L_p = \lambda_0/\text{Im}(n_{\text{eff}})$, where λ_0 is the vacuum wavelength and $\text{Im}(n_{\text{eff}})$ is the imaginary part of the effective refractive index. The normalized mode area is defined as A_{eff}/A_0 , where $A_0 = \lambda_0^2/4$ is the diffraction limit mode area and the effective mode area, which reflects the mode confinement ability of waveguide, is defined as:

$$A_{\text{eff}} = \iint |E|^2 dx dy$$

5

where W is the electromagnetic energy density [47–48]. In order to better describe the relationship between the mode propagation length and the normalized mode area, the figure of merit is defined as $F_0/M = \text{Re}(n_{\text{eff}}) / \text{Im}(n_{\text{eff}})$ [49].

3 Results And Discussions

Figure 2 (a) - (f) show the mode profiles of the electric field $|E|$ of the fundamental mode of the waveguide structure when the air core size in the nanotube/dielectric substrate and the gap height between the nanotube and dielectric substrate are different. Here, the parameters are $f_0=30\text{Thz}$, $\mu_c = 0.5\text{eV}$, $w_0=200\text{nm}$,

$h_0=100\text{nm}$, $r_0=30\text{nm}$, $\varepsilon_1 = 1$, $\varepsilon_2 = 2.09$. Meanwhile, when $S_1=S_2=0$, the waveguide structure is similar to the structure proposed in reference [40]. It can be seen from Figure 2 that most of the electromagnetic energy is confined to the gap between the nanotube and the dielectric substrate, and the mode field confinement is very strong. As the air core size increases, the electromagnetic energy gradually diffuses from the gap between the nanotube and the dielectric substrate to the periphery of the nanotube, which will lead to weak mode field confinement and low mode propagation loss. In addition, it can be seen that with the increase of gap height g , the size of electromagnetic field distributed in the gap will increase, and the mode area will also increase, but the propagation loss decreases, resulting in the increase of propagation length.

The dependences of the mode properties on the ratio S_1 are shown in figures 3 under different S_2 . As shown in Fig. 3(a), when S_2 is fixed, the effective mode index $\text{Re}(n_{\text{eff}})$ decreases slowly with increasing S_1 . As S_1 increases, the propagation length L_m increases monotonically, and the normalized mode field area A_{eff}/A_0 also increases monotonically, but the variation range is very small. Since the propagation length increases faster than the normalized mode area, the figure of merit increases slowly. At the same time, it can be seen that when S_1 is small, the change of mode properties is slow, but when S_1 is large, the change of mode properties is fast. This is because when S_1 is large, the electromagnetic field will diffuse to the dielectric layer around the nanotube, the mode confinement becomes worse, and the mode loss decreases faster. That is to say, when $S_2 = 0, 0.3$, the change of mode properties is close; when $S_2 = 0.6, 0.9$, the propagation length and normalized mode area change more. Especially, when $S_1 = S_2 = 0$, the waveguide mode properties are similar to those mentioned in reference [40]. It can be seen from Fig. 3 that when both S_1 and S_2 are greater than 0, the propagation length and the figure of merit of the proposed waveguide are higher than those in reference [40], and the normalized mode field area does not increase much than that in reference [40]. Therefore, it can be said that within a certain parameter range, the mode properties of the proposed structure are better than those in reference [40].

The fundamental mode properties of the waveguide structure as a function of the gap height g are depicted in Fig. 4. When g gradually increases, the coupling between graphene nanotubes and dielectric substrate decreases, resulting in the decrease of effective mode index $\text{Re}(n_{\text{eff}})$. Increasing the gap height leads to a larger mode area and weaker confinement. At the same time, the mode propagation loss decreases with increasing g , resulting in a longer propagation length. According to Fig. 4 (d), FOM first increases and then tends to be flat. Therefore, the increase of g can appropriately improve the waveguide performance, but too large g has little effect on the waveguide performance. Taking into account the propagation length and the mode area, $g=20\text{nm}$ is selected for the following research.

Another geometry parameter relating to the mode properties is the outer radius r_0 of the nanotube. The dependences of the mode properties on parameter r_0 are shown in figures 5, where r_0 varies from 30 nm to 100 nm. As can be seen from Fig. 5 (a), $\text{Re}(n_{\text{eff}})$ first decreases and then increases with increasing r_0 . The normalized mode area increases first and then decreases with increasing r_0 , and the later change range is small, indicating that when r_0 is large ($r_0 > 80\text{nm}$), r_0 has little effect on the mode field

confinement. Moreover, as r_o increases, both L_m and FOM gradually decrease, and the variation range is large, as shown in Fig. 4 (b) and 4 (d). This is due to the fact that increasing the outer radius r_o of the nanotube can increase the surface area of the graphene layer, so the mode propagation loss increases and the propagation distance decreases. It can be seen from the above when r_o is the smallest, the mode properties are the best, and the figure of merit is the highest with the longest propagation length and the smallest normalized mold area. However, considering the difficulty of manufacturing, r_o should not be too small. Therefore, $r_o=30\text{nm}$ is selected for the following study in this paper.

The permittivity ε_2 of nanotube/dielectric substrate also has a great influence on the waveguide performance. Fig. 6 shows the dependence of the mode properties on the permittivity ε_2 , where ε_2 increases from 2 to 8. In Fig. 6(a), we can see that increasing ε_2 the effective mode index $\text{Re}(n_{\text{eff}})$ increases linearly and the mode propagation loss also increases, resulting in a smaller propagation length L_m , as shown in Fig. 6(b). As can be seen in Figure 6 (c), as ε_2 increases, the normalized mode area decreases gradually and the maximum variation range of normalized mode area is about $1 \times 10^{-7} \sim 6 \times 10^{-7}$, meaning that the field confinement is very tight. Figure 6(d) depicts the dependence of the figure of merit FOM on the permittivity ε_2 , and it can be seen that the smaller the permittivity ε_2 , the higher the figure of merit FOM, and the better the mode properties. Therefore, the permittivity of nanotube/dielectric substrate should be as small as possible in application. SiO_2 with the permittivity $\varepsilon_2 = 2.09$ is selected as the filling medium in this paper [50].

Compared to noble metals, the greatest advantage of the graphene is that the graphene conductivity can be dynamically tuned when its geometric structure is fixed [51]. Fig. 7 shows the dependence of mode properties on frequency f_0 under different chemical potentials. It can be seen that as f_0 increases, for four different chemical potentials μ_c , $\text{Re}(n_{\text{eff}})$ increases gradually, L_m decreases gradually, and the normalized mode field area is complex, but it varied little. FOM gradually increases with increasing f_0 . As can be seen from Fig. 7(a) and (c), when f_0 is fixed, as μ_c increases, $\text{Re}(n_{\text{eff}})$ decreases and the normalized mode field area increases due to the weak field confinement. At the same time, as μ_c increases, the carrier relaxation time increases, which reduces the inherent loss of graphene, so L_m increases, as shown in Fig. 7 (b). Because the propagation length increases faster than the mode field area, FOM also increases by f_0 , as shown in Fig. 7 (d). For example, when $\mu_c = 0.5\text{eV}$ and $f_0=20\text{Tz}$, the propagation length and normalized mode area are $12.56\mu\text{m}$ and 6.6×10^{-7} respectively. Compared with the research in related fields, the proposed waveguide has the smaller normalized mold area ($\sim 10^{-7}$). In the case of the same propagation length, the normalized mold area of the waveguide proposed in this paper is two orders of magnitude smaller than that of the graphene-coated nanowire waveguide with the dielectric substrate ($\sim 10^{-5}$) [40]. And the normalized mold area of the waveguide proposed is one order of magnitude smaller than that of the triangular-shaped graphene-coated nanowires on substrate ($\sim 10^{-6}$) [41].

4 Conclusions

A graphene-coated nanotube plasmon waveguide structure with a dielectric substrate is designed and its transmission properties are studied in detail. The results have revealed that the structure proposed in this paper has better mode properties than that proposed in reference [40] when the appropriate parameters are selected. The smaller the outer diameter of the nanotube, the longer the propagation length, the smaller the mode area, and the better the mode properties; meanwhile, it is shown that the waveguide structure can locally break through the restrictive relationship between surface plasmon mode loss and mode area, that is, the mode loss and mode area are reduced at the same time. The larger the gap height is, the better the mode properties are, but the mode properties are basically unchanged when the gap height is too large. Reducing the permittivity of nanotube or increasing the chemical potential of graphene can improve the figure of merit. In particular, the proposed waveguide can realize the propagation distance in the order of $\sim \mu\text{m}$, and the normalized mode area is compressed to $\sim 10^{-7}$. This structure has important applications in the field of deep sub-wavelength transmission and integrated nanophotonic devices.

Declarations

1. Funding

This work was supported by Chongqing higher education teaching reform research project (Grant numbers [213143]). Author Miao Sun has received research support from Chongqing Normal University.

2. Competing Interests

Financial interests: Author Miao Sun, Zhuanling He and Libing Huang declare they have no financial interests.

The authors have no relevant financial or non-financial interests to disclose.

3. Author Contributions

All authors contributed to the study conception and design. Material preparation, data collection and analysis were performed by Miao Sun, Zhuanling He and Libing Huang. The first draft of the manuscript was written by Miao Sun and all authors commented on previous versions of the manuscript. All authors read and approved the final manuscript.

4. Data Availability

The datasets generated during and analysed during the current study are available from the corresponding author on reasonable request.

References

1. Gramotnev, D. K., Bozhevolnyi, S. I.: Plasmonics beyond the diffraction limit. *Nat. Photonics* 4(2), 83-91 (2010). <https://doi.org/1038/nphoton.2009.282>
2. Li P.: Research progress of plasmonic nanofocusing. *Acta Physica Sinica* 68(14): 146201 (2019). <https://doi.org/7498/aps.68.20190564>
3. Liu John S. Q., Pala Ragip A., Afshinmanesh Farzaneh, Cai Wenshan, Brongersma M-ark L.: A submicron plasmonic dichroic splitter. *Nat. Commun.* 2, 525 (2011). <https://org/10.1038/ncomms1537>.
4. Roszkiewicz A., Nasalski W.: Reflection suppression and absorption enhancement of optical field at thin metal gratings with narrow slits. *Opt. Lett.* 37, 3759 (2012). <https://doi.org/10.1364/OL.37.003759>
5. Heiss D., Dolores-Calzadilla V., Fiore A., et al.: Integrated Photonics Research, Silicon and Nanophotonics. Optical Society of America. IM2A 3 (2013). <https://doi.org/1364/IPRSN.2013.IM2A.3>.
6. Dolores-Calzadilla V., Heiss D., Smit M.: Realization of efficient metal grating couplers for membrane-based integrated photonics. *Opt. Lett.* 40, 2755 (2015). <https://doi.org/1364/OL.40.002755>.
7. Lu C., Liu Y. C., Hu X., et al.: Integrated ultracompact and broadband wavelength demultiplexer based on multi-component nano-cavities. *Sci. Rep.* 6, 27428 (2016). <https://doi.org/1038/srep27428>
8. Teng D., Wang K., Li Z., et al.: Graphene-coated nanowire dimers for deep subwavelength waveguiding in mid-infrared range. *Opt. Express* 27(9), 12458-12469 (2019). <https://doi.org/1364/OE.27.012458>
9. Berini P.: Plasmon polariton modes guided by a metal film of finite width. *Opt. Lett.* 15, 1011-1013 (1999). <https://doi.org/1364/ol.24.001011>
10. Wang Y., Ma Y., Guo X., et al.: Single-mode plasmonic waveguiding properties of metal nanowires with dielectric substrates. *Opt. Express* 20(17), 19006-19015 (2012). <https://doi.org/1364/OE.20.019006>
11. Wei H., Pan D., Zhang S., et al.: Plasmon waveguiding in nanowires. *Chem. Rev.* 118(6), 2882-2926 (2018). <https://doi.org/10.1021/acs.chemrev.7b00441>
12. Pile D. F. P., Ogawa T.: Theoretical and experimental investigation of strongly localized plasmon on triangular metal wedges for subwavelength wave guiding. *Appl. Phys. Lett.* 87(6), 061106 (2005). <https://doi.org/1063/1.1991990>
13. Veronis G., Fan S.: Guided subwavelength plasmonic mode supported by a slot in a thin metal film. *Opt. Lett.* 30: 3359-3361(2005). <https://doi.org/1364/ol.30.003359>
14. Moreno E., Rodrigo S. G., Bozhevolnyi S. I., et al.: Guiding and focusing of electromagnetic fields with wedge plasmon polaritons. *Phys. Rev. Lett.* 100(2), 023901 (2008). <https://doi.org/1103/PhysRevLett.100.023901>
15. Tanaka K., Tanaka M.: Simulations of nanometric optical circuits based on surface plasmon polariton gap waveguide. *Appl. Phys. Lett.* 8, 1158-1160 (2003). <https://doi.org/1063/1.1557323>

16. Chen Y., Xu J., Shi N., et al.: Mode properties of metal-insulator-metal waveguide bragg grating. *Acta Optica Sinica*. 37(11), 1123002 (2017). <https://doi.org/10.3788/aos201737.1123002>
17. Bozhevolnyi S. I., Volkov V. S., Devaux E., et al.: Channel plasmon-polariton guiding by subwavelength metal grooves. *Phys. Rev. Lett.* 4, 1-4 (2005). <https://doi.org/10.1103/PhysRevLett.95.046802>
18. Lee I. M., Jung J., Park J. H., et al.: Dispersion characteristics of channel plasmon polariton waveguides with step trench type grooves. *Opt. Express* 25, 16596-16603 (2007). <https://doi.org/10.1364/OE.15.016596>
19. Reinhardt C., Passinger S., Chichkov B. N., et al.: Laser-fabricated dielectric optical components for surface Plasmon polaritons. *Opt. Lett.* 31, 1307-1309 (2006). <https://doi.org/10.1364/ol.31.001307>
20. Chen Y. T., Vladimir A. Z., et al.: Efficient interfacing photonic and long-range dielectric-loaded plasmonic waveguides. *Opt. Express* 23, 9100-9108 (2015). <https://doi.org/10.1364/OE.23.009100>
21. Shao X., Zhang G., Wang Q., et al.: Transmission characteristics of long-range dielectric-loaded surface plasmon polariton waveguide based on golden ratio. *Laser Optoelectron. Prog.* 53(6), 061301 (2016). <https://doi.org/10.3788/lop53.061301>
22. Oulton R. F., Sorger V. J., Genov D. A., et al.: A hybrid plasmonic waveguide for subwavelength confinement and long-range propagation. *Nat. Photonics* 2, 496-500 (2008). <https://doi.org/10.1038/nphoton.2008.131>
23. Bian Y., Zheng Z., Zhao X., et al.: Symmetric hybrid surface plasmon polariton waveguides for 3D photonic integration. *Opt. Express* 17(23), 21320-21325 (2009). <https://doi.org/10.1364/OE.17.021320>
24. Gao Y., Shadrivov I. V.: Second harmonic generation in graphene-coated nanowires. *Opt. Lett.* 41(15), 3623-3626 (2016). <https://doi.org/10.1364/OL.41.003623>
25. Vakil A., Engheta N.: Transformation optics using graphene. *Science*. 332(6035), 1291-1294 (2011). <https://doi.org/10.1126/science.1202691>
26. Wang F., Zhang Y. B., Tian C. S., et al.: Gate-tunable Optical Transitions in Graphene. *Science*. 320, 206 (2008). <https://doi.org/10.1126/science.1152793>
27. Koppens F. H. L., Chang D. E., Garcia de Abajo F. J.: Graphene Plasmonics: A Platform for Strong Light-Matter Interactions. *Nano Lett.* 11, 3370 (2011). <https://doi.org/10.1021/nl201771h>
28. Lu H., Zhao J., Gu M.: Nanowire-assisted excitation and propagation of mid-infrared surface plasmon polaritons in graphene. *J. Appl. Phys.* 120(16), 163106 (2016). <https://doi.org/10.1063/1.4966600>
29. Ooi K. J. A., Chu H. S., Ang L. K., et al.: Mid-infrared Active Graphene Nanoribbon Plasmonic Waveguide Devices. *J Opt Soc Am B*. 30(12), 3111-3116 (2013). <https://doi.org/10.1364/JOSAB.30.003111>
30. He X., Zhang X., Zhang H., et al.: Graphene Covered on Microfiber Exhibiting Polarization and Polarization-dependent Saturable Absorption. *IEEE J Sel Top Quantum Electron*. 20(1), 4500107 (2014). <https://doi.org/10.1109/JSTQE.2013.2270278>

31. Wu Y., Yao B., Zhang A., et al.: Graphene-coated Microfiber Bragg Grating for High- sensitivity Gas Sensing. *Opt. Lett.* 39(5), 1235-1237 (2014). <https://doi.org/10.1364/OL.39.001235>
32. Liu P., Zhang X., Ma Z., et al.: Surface plasmon modes in graphene wedge and groove waveguides. *Opt. Express* 21(26), 32432-32440 (2013). <https://doi.org/10.1364/OE.21.032432>
33. Sheng P., Chen M., Cai J., et al.: A hybrid graphene surface plasmon waveguide. *Journal of Guilin University of Electronic Science and Technology*. 36(02), 94-98 (2016). <https://doi.org/10.16725/j.cnki.cn45-1351/tn.2016.02.002>
34. Sun Miao, Tian J., Lan X., et al.: Transmission properties of two vertically coupled double-graphene-coated nanowires integrated with substrate. *Optik*. 185 (2019). <https://doi.org/10.1016/j.ijleo.2019.03.090>
35. Li Z., Feng D., Li X., et al.: Graphene surface plasmon polaritons based photoelectric modulator with double branched structure. *Acta Optica Sinica*. 38(1), 0124001 (2018). <https://doi.org/10.3788/aos201838.0124001>
36. Li W., Chen B., Meng C., et al.: Ultrafast all-optical graphene modulator. *Nano Lett.* 14(2): 955-959 (2014). <https://doi.org/10.1021/nl404356t>
37. Gao Y., Ren G., Zhu B., et al.: Analytical model for plasmon modes in graphene-coated nanowire. *Opt. Express* 22(20), 24322-24331 (2014). <https://doi.org/10.1364/OE.22.024322>
38. Yang J. F., Yang J. J., Deng W., et al.: Transmission Properties and Molecular Sensing Application of CGPW. *Opt. Express* 23(25), 32289-32291 (2015). <https://doi.org/10.1364/OE.23.032289>
39. Liu J. P., Zhai X., Wang L. L., et al.: Analysis of mid-infrared surface plasmon modes in a graphene-based cylindrical hybrid waveguide. *Plasmonics*. 11(3), 703-711 (2016). <https://doi.org/10.1007/s11468-015-0095-z>
40. Hajati M., Hajati Y.: Deep Subwavelength Confinement of Mid-infrared Plasmon Modes by Coupling Graphene-Coated Nanowire with a Dielectric Substrate. *Plasmonics*. 13(2) (2018). <https://doi.org/10.1007/s11468-017-0524-2>
41. Teng D., Ma W., Yang Y., et al.: Study on Subwavelength Transmission Properties of Triangular-Shaped Graphene-Coated Nanowires on Substrate. *Acta Optica Sinica*. 40(13), 181-188 (2020). <https://doi.org/10.3788/aos202040.1324002>
42. Wu D., Tian J. P., Yang R. C.: Study of mode performances of graphene coated nanowire integrated with triangle edge substrate. *J. Nonlinear Opt. Phys. Mater.* 27(2), 1850013 (2018). <https://doi.org/10.1142/S0218863518500133>
43. Yang J. F., Yang J. J., Deng W., et al.: Transmission properties and molecular sensing application of CGPW. *Opt. Express*. 23, 32289 (2015). <https://doi.org/10.1364/OE.23.032289>
44. Nikitin Y. A., Guinea F., Garcia-Vidal F. J., et al.: Fields radiated by a nano emitter in a graphene sheet. *Phys. Rev. B*. 84, 195446 (2011). <https://doi.org/10.1103/PhysRevB.84.195446>
45. Francescato Y., Giannini V., and Maier S. A.: Strongly confined gap plasmon modes in graphene sandwiches and graphene-on-silicon. *New J. Phys.* 15, 063020 (2013). <https://doi.org/10.1088/1367-2630/15/6/063020>

46. Hajati M., Hajati Y.: Plasmonic characteristics of two vertically coupled graphene-coated nanowires integrated with substrate. *Appl. Opt.* 56, 870 (2017). <https://doi.org/10.1364/AO.56.000870>
47. Wang Y., Ma Y., Guo X., et al.: Single-mode plasmonic waveguiding properties of metal nanowires with dielectric substrates. *Opt. Express*. 20, 19006 (2012). <https://doi.org/10.1364/OE.20.019006>
48. Oulton R. F., Sorger V. J., Genov D. A., et al.: A hybrid plasmonic waveguide for subwavelength confinement and long-range propagation. *Nat. Photonics* 2(8), 496-500 (2008). <https://doi.org/10.1038/nphoton.2008.131>
49. Berini.: Figures of merit for surface plasmon waveguides. *Opt. Express*, 14, 13030 (2006). <https://doi.org/10.1364/OE.14.013030>
50. He S., Zhang X., He Y.: Graphene nano-ribbon waveguides of record-small mode area and ultra-high effective refractive indices for future VLSI. *Opt. Express* 21(25), 30664-30673 (2013). <https://doi.org/10.1364/OE.21.030664>
51. Wu X. T.: Study on the transmission properties of nano-scale optical device based on graphene. Taiyuan: Shanxi University. 31-36 (2018).

Figures

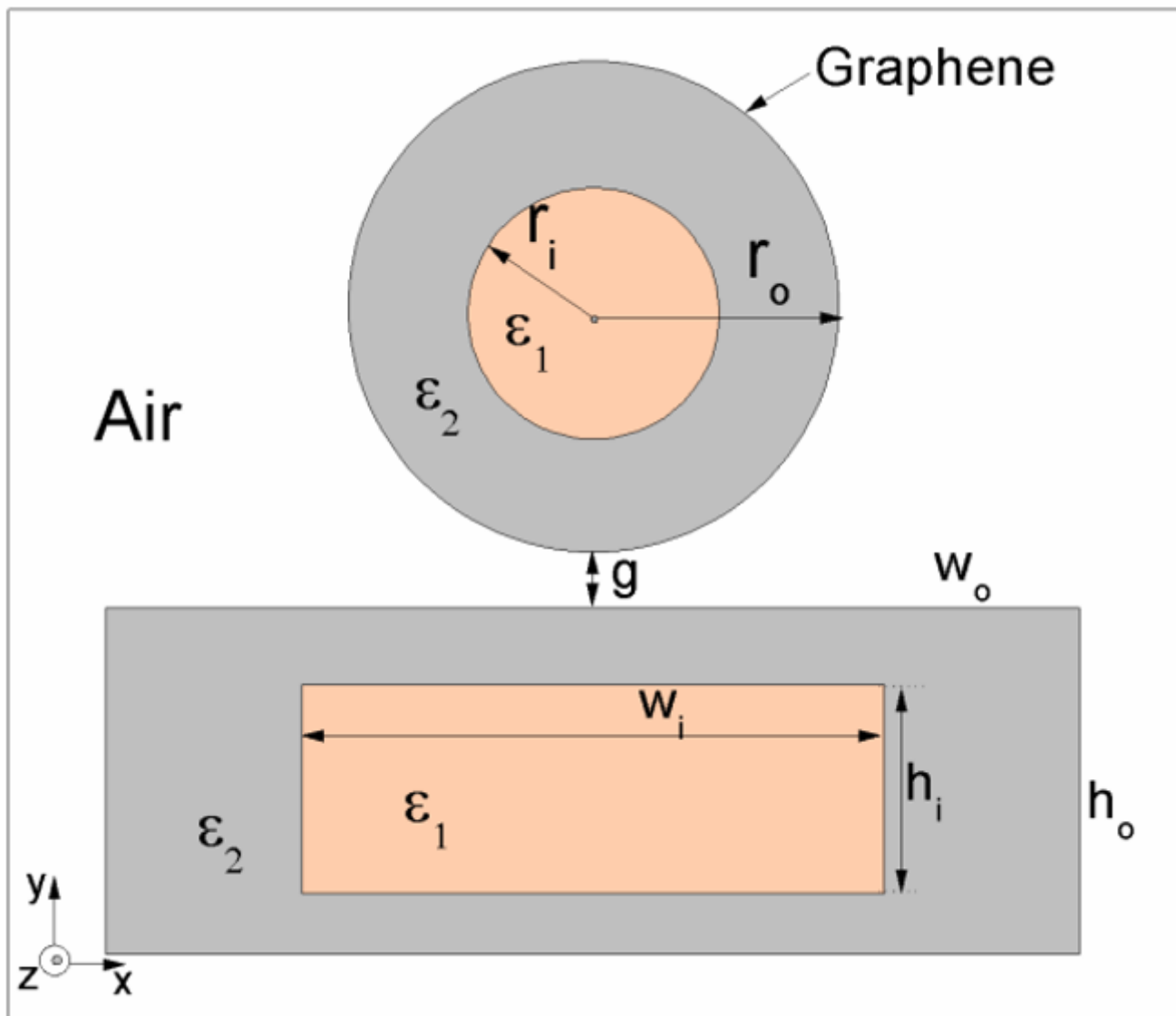


Figure 1

Schematic of the plasmonic waveguide

Figure 2

Normalized electric field mode distributions of the fundamental mode. (a) $g=5\text{nm}$, $S_1=S_2=0$; (b) $g=5\text{nm}$, $S_1=S_2=0.4$; (c) $g=5\text{nm}$, $S_1=S_2=0.8$; (d) $g=15\text{nm}$, $S_1=S_2=0$; (e) $g=15\text{nm}$, $S_1=S_2=0.4$; (f) $g=15\text{nm}$, $S_1=S_2=0.8$

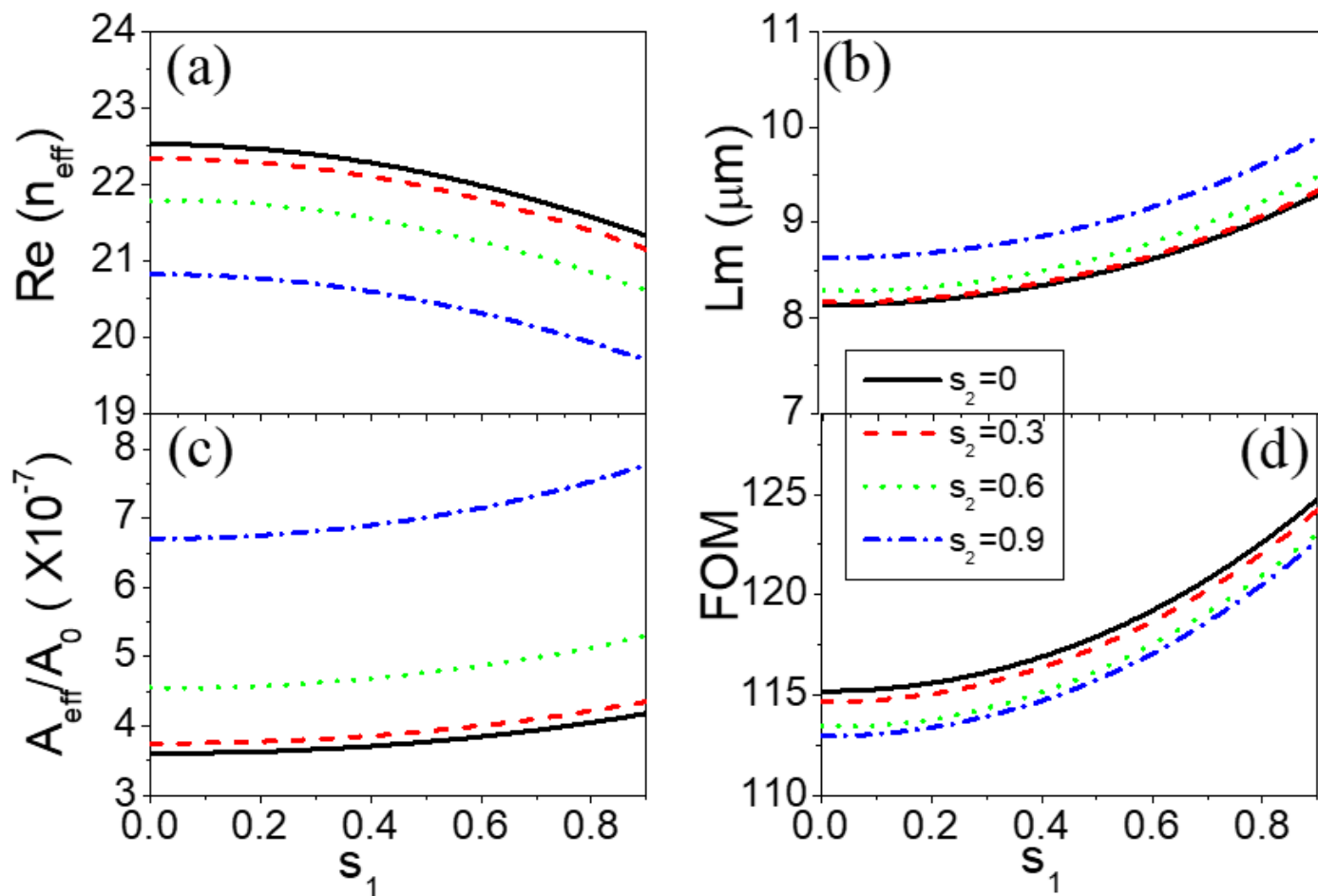


Figure 3

Dependence of modal properties on S_1 . (a) Effective mode index $\text{Re}(n_{\text{eff}})$; (b) Propagation length L_m ; (c) Normalized mode area A_{eff}/A_0 ; (d) Figure of merit FOM. Here, $f_0=30\text{THz}$, $\mu_c=0.5\text{eV}$, $\epsilon_1=1$, $\epsilon_2=2.09$, $g=10\text{nm}$, $r_o=30\text{nm}$, $w_o=200\text{nm}$, $h_o=100\text{nm}$, $S_2=0, 0.3, 0.6, 0.9$

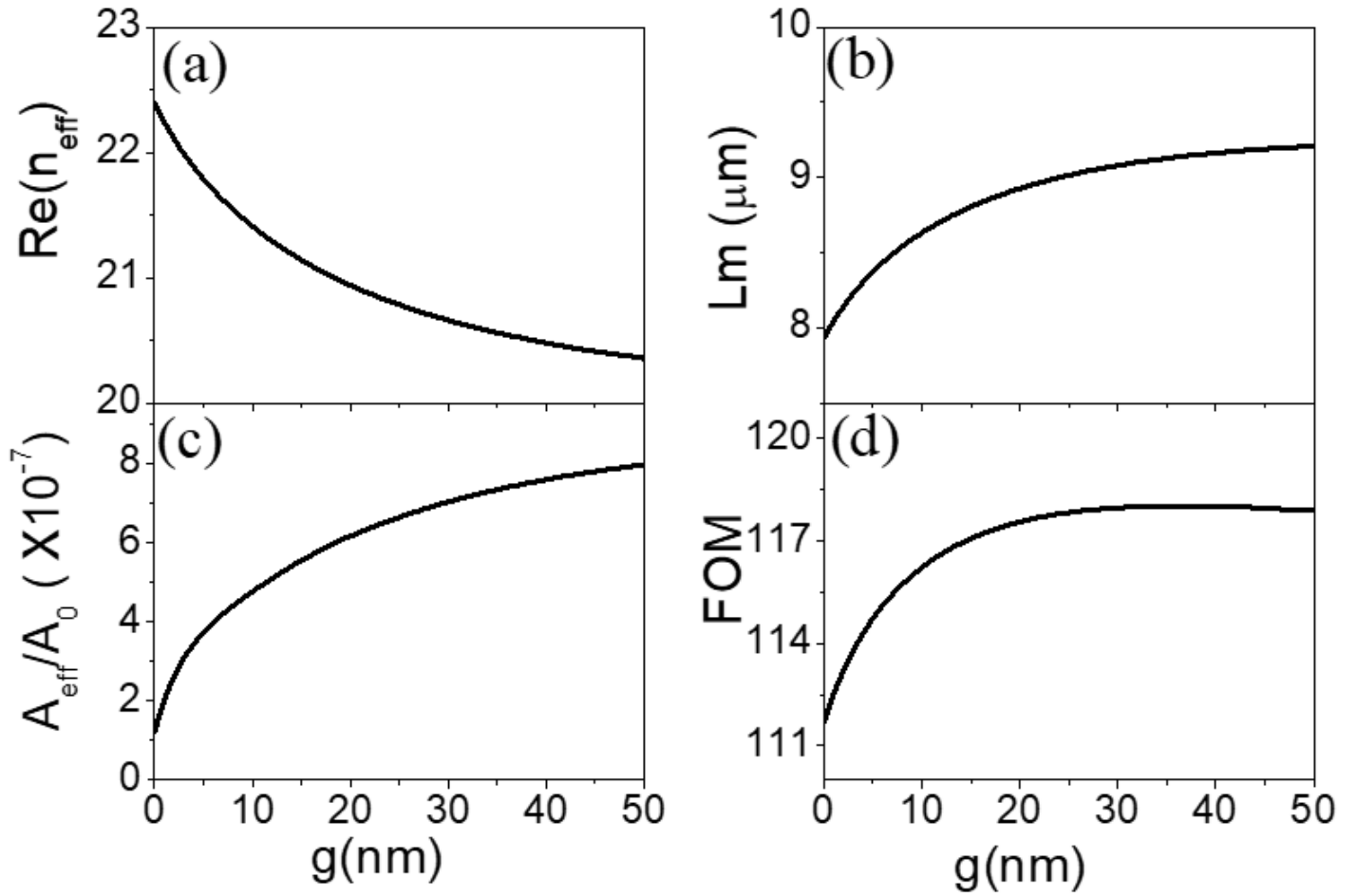


Figure 4

Dependence of modal properties on gap height g . (a) Effective mode index $\text{Re}(n_{\text{eff}})$; (b) Propagation length L_m ; (c) Normalized mode area A_{eff}/A_0 ; (d) Figure of merit FOM. Here, $f_0=30\text{THz}$, $\mu_c=0.5\text{eV}$, $\epsilon_1=1$, $\epsilon_2=2.09$, $r_0=30\text{nm}$, $w_0=200\text{nm}$, $h_0=100\text{nm}$, $S_1=0.5$, $S_2=0.6$

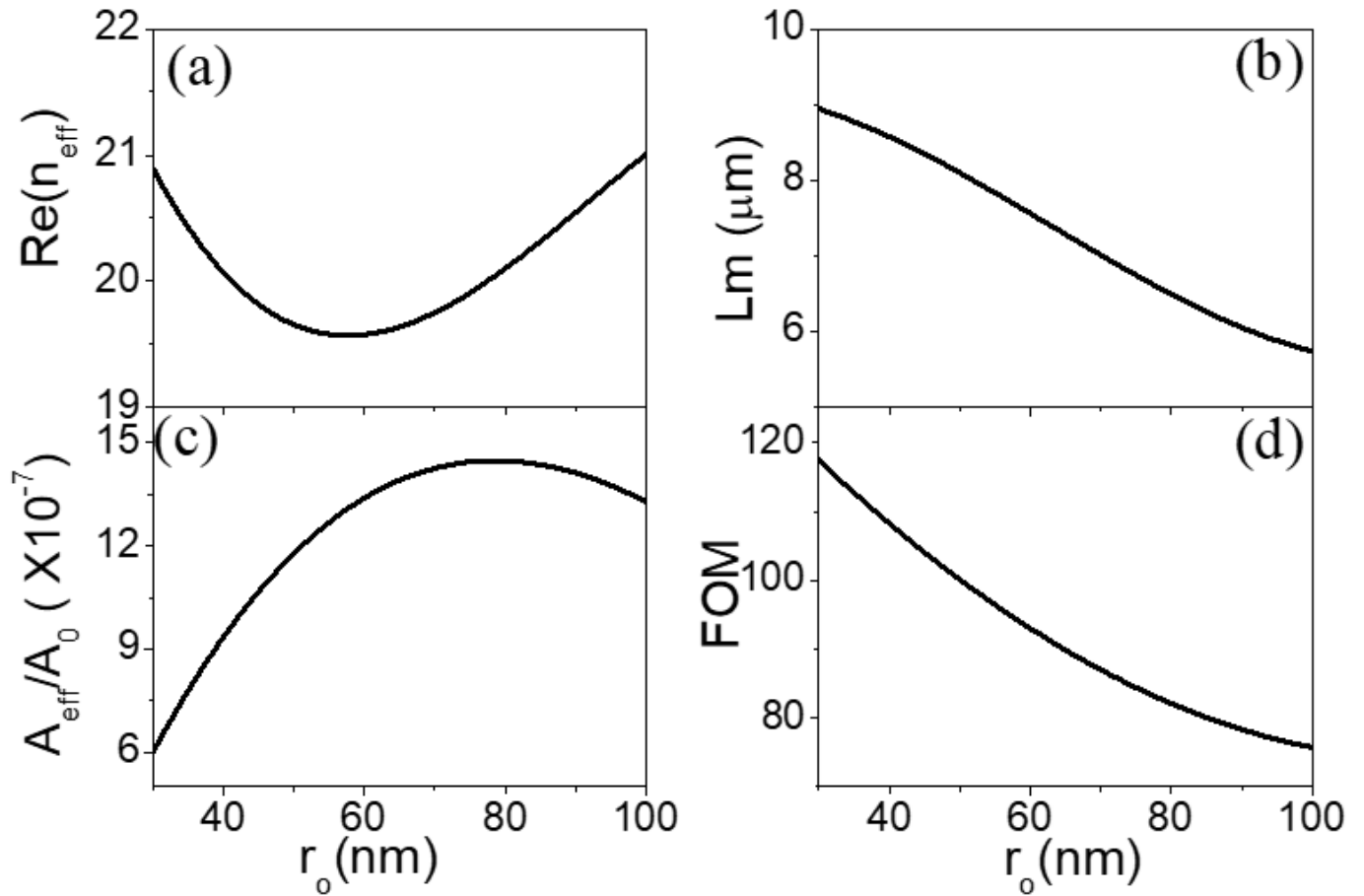


Figure 5

Dependence of modal properties on outer radius of nanotube r_o . (a) Effective mode index $\text{Re}(n_{\text{eff}})$; (b) Propagation length L_m ; (c) Normalized mode area A_{eff}/A_0 ; (d) Figure of merit FOM. Here, $f_0=30\text{THz}$, $\mu_c=0.5\text{eV}$, $\epsilon_1=1$, $\epsilon_2=2.09$, $g=20\text{nm}$, $w_0=200\text{nm}$, $h_0=100\text{nm}$, $S_1=0.5$, $S_2=0.6$

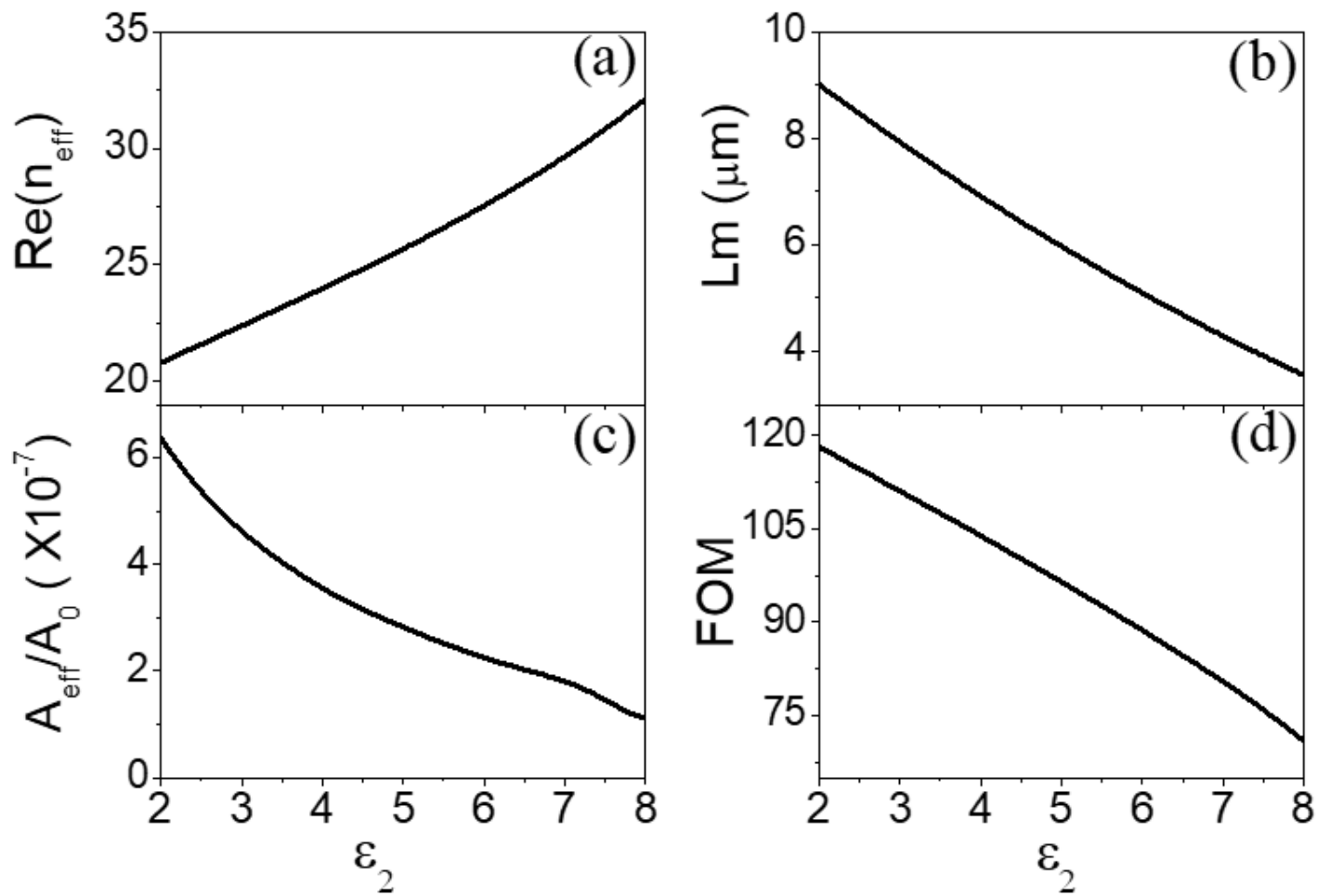


Figure 6

Dependence of modal properties on permittivity of nanotube and dielectric substrate ϵ_2 . (a) Effective mode index $\text{Re}(n_{\text{eff}})$; (b) Propagation length L_m ; (c) Normalized mode area A_{eff}/A_0 ; (d) Figure of merit FOM. Here, $f_0=30\text{THz}$, $\mu_c=0.5\text{eV}$, $\epsilon_1=1$, $g=20\text{nm}$, $r_0=30\text{nm}$, $w_0=200\text{nm}$, $h_0=100\text{nm}$, $S_1=0.5$, $S_2=0.6$

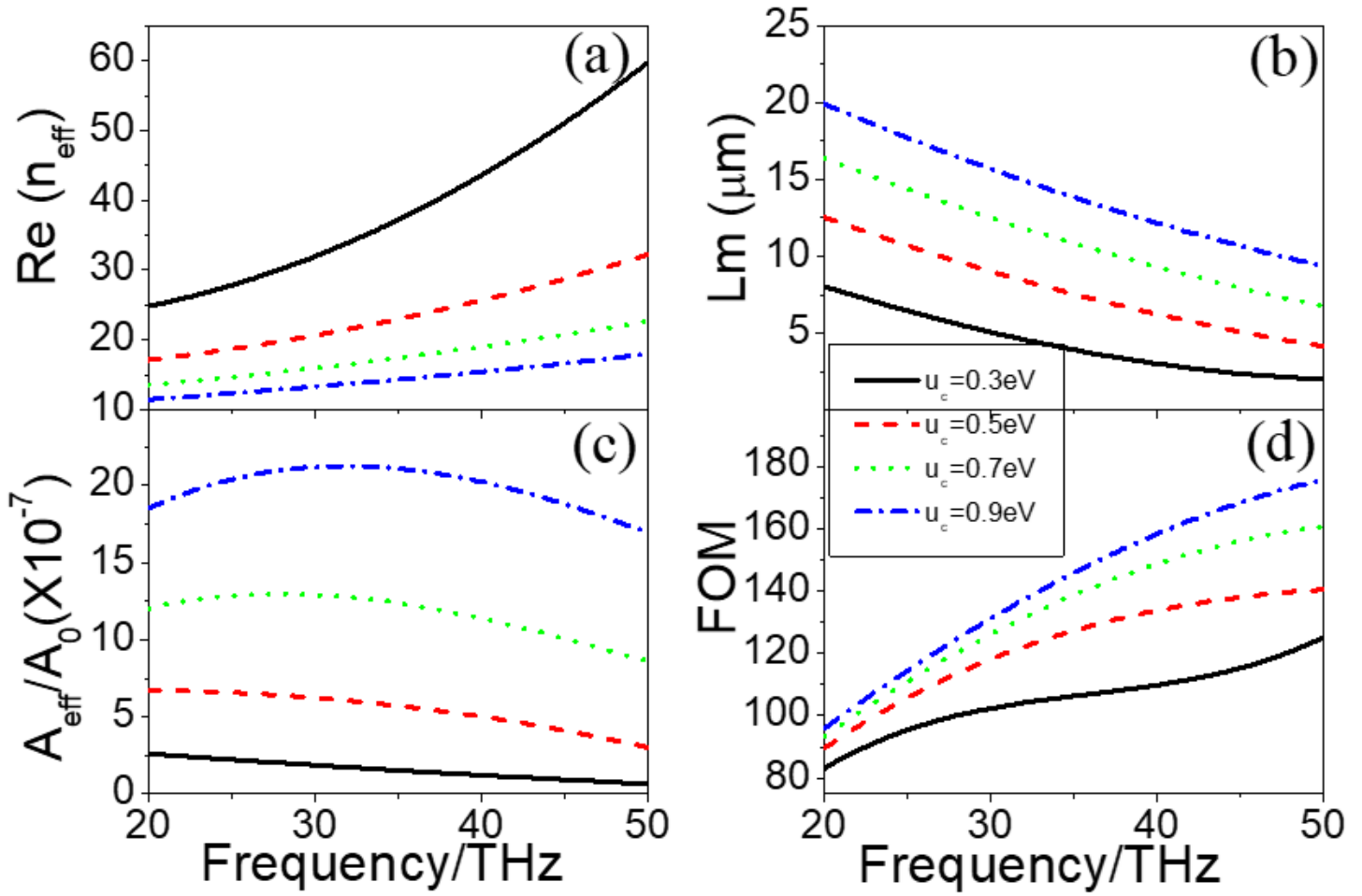


Figure 7

Dependence of modal properties on frequency f_0 . (a) Effective mode index $\text{Re}(n_{\text{eff}})$; (b) Propagation length L_m ; (c) Normalized mode area A_{eff}/A_0 ; (d) Figure of merit FOM. Here, $r_o=30\text{nm}$, $g=20\text{nm}$, $w_o=200\text{nm}$, $h_o=100\text{nm}$, $S_1=0.5$, $S_2=0.6$, $\mu_c=0.3\text{eV}, 0.5\text{eV}, 0.7\text{eV}, 0.9\text{eV}$